

SUPPORTING INFORMATION

Complementarity of Density Functional Theory and Nuclear Magnetic Resonance Tools To Probe the Nano-Layered Silicates Surface Chemistry and Morphology

Mathilde Poirier^{1*}, Yannick Millot², Elisa Silva Gomes², Maguy Jaber³, Virginie Herledan²,
Guillaume Laugel², Pierre Micoud¹, François Martin¹, H el ene Lauron-Pernot² and Herv e
Toulhoat^{2*}

¹ ERT G eomat eriaux, GET, Universit e de Toulouse, CNRS, IRD, UPS, 14 Avenue Edouard
Belin ; 31400 Toulouse, France

² Laboratoire de R eactivit e de Surface UMR 7197 Sorbonne Universit e-CNRS, UPMC, 4 Place
Jussieu ; 75005 Paris, France

³ Laboratoire d'Arch eologie Mol eculaire et Structurale UMR 8220 Sorbonne Universit es-
CNRS, UPMC, 4 Place Jussieu ; 75005 Paris, France

* mathilde.l.poirier@gmail.com; (+33)787038049

* herve.toulhoat@orange.fr; (+33)67276655

1 - Supporting Tables	3
Table S1: DLS size distribution of the series of nano-sized synthetic talc samples	3
2 – Supporting Figures	4
Figure S1: SEM images of the nano-sized talc samples with increasing crystallinity.....	4
Figure S2: ^1H direct polarization MAS NMR spectrum of sodium acetate.....	6
Figure S3: $\{^1\text{H}\} - ^{13}\text{C}$ HETCOR spectra of ST-AcONa.....	6
Figure S4: Example of deconvolution of a ^1H DP MAS-NMR	7
Figure S5: Slab model for the fully hydrated (130) talc edge: (a) side view, (b) top view, (c) front view, (d) perspective view.....	8
Figure S6: Slab model for the fully hydrated (100) talc edge: (a) side view, (b) top view, (c) front view, (d) perspective view.....	9
Figure S7: ^1H DQ-SQ PC7 spectrum of ST-6H.....	10
Figure S8: Decompositions of ^{29}Si NMR chemical shifts profiles	11
Figure S9: Variation of Log-normal talc nanoparticle size distributions parameters with synthesis time.....	14
<i>Figure S9a: Variation of the mean talc nanoparticle thickness with synthesis time.</i>	14
<i>Figure S9b: Variation of the log-normal distribution parameter μ with time of synthesis</i>	14
Figure S10: Example of lognormal distribution fitting DLS data of ST-2W.....	15
3 – Supporting calculations	16
3-1 Calculation of the hydrodynamic radius of a talc nanocrystallite at equilibrium morphology	16

1 - Supporting Tables

Table S1: DLS size distribution of the series of nano-sized synthetic talc samples.

This table presents the dispersion data obtained by DLS analysis on the series of synthetic talc samples. The corresponding D50 values are reported in Table 1. Short synthesis time samples display a homogeneous particle size distribution centered on the D50 value. The distribution tends to widen when the synthesis time increases (for example, ST-1M contains synthetic talc nanoparticles of about 171 nm (D50) with a size dispersion ranging from 156 nm to almost 2 μm).

ST-2H		ST-6H		ST-1D		ST-2W		ST-1M	
Size (nm)	Number	Size (nm)	Number	Size (nm)	Number	Size (nm)	Number	Size (nm)	Number
12.84	0.14	17.74	0.39	37.18	0.82	112.77	0.23	155.87	0.41
14.08	0.29	20.38	0.2	61.83	0.06	129.55	0.39	170.97	0.31
14.75	0.07	22.36	0.12	74.39	0.05	163.25	0.04	259.21	0.07
15.44	0.24	25.68	0.06	85.45	0.03	170.97	0.12	271.48	0.07
16.17	0.09	26.9	0.05	93.73	0.01	179.07	0.04	392.99	0.11
17.74	0.09	28.17	0.03	107.68	0.01	187.54	0.06	1982.39	0.01
18.58	0.04	29.5	0.06			196.41	0.04		
19.46	0.02	30.9	0.03			205.71	0.02		
21.35	0.01	32.36	0.04			247.5	0.01		
22.36	0.01	33.89	0.02			786.29	0.02		
24.52	0.01	37.18	0.01			862.47	0.01		
						946.03	0.01		

2 – Supporting Figures

Figure S1: SEM images of the nano-sized talc samples with increasing crystallinity.

SEM investigations were performed at the Centre de Micro-Caractérisation Raimond Castaing of Toulouse (France) on a MEB-FEG JEOL JSM 7800F Prime apparatus equipped with a back-scattered electron detector. The images were recorded under a 3 kV or 10 kV voltage on carbon-metallized talc powders. The results evidence lamellar platelets of growing size when the duration of synthesis increases (from a dozen of nm for ST-2H to around 1 μm for ST-1M). For a fraction of particles, the increase of the synthesis time does not lead to an increase of the particle size. This is particularly noticeable in ST-2W and ST-1M where some of the particles are large (about 1 μm), while most of them remained blocked at the nano-sized range (around 100 nm).

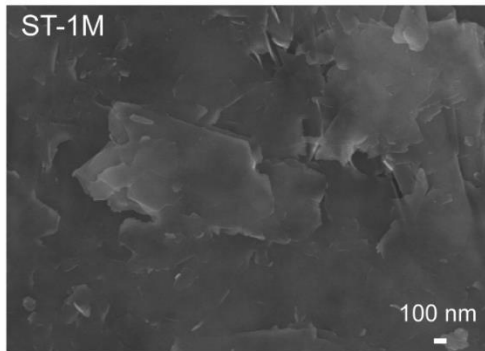
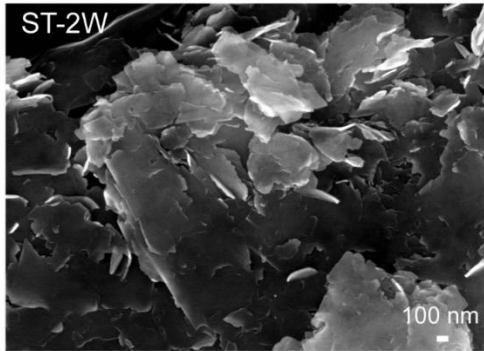
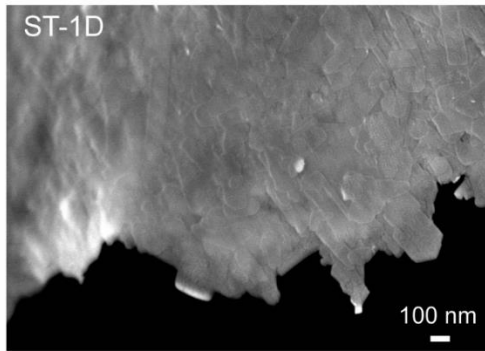
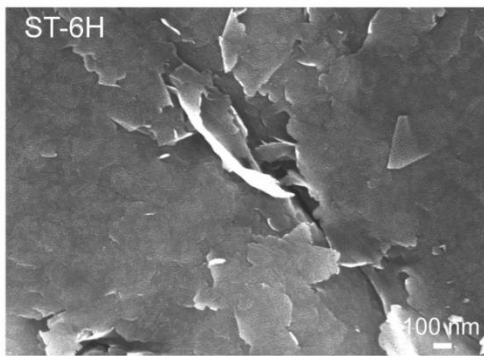
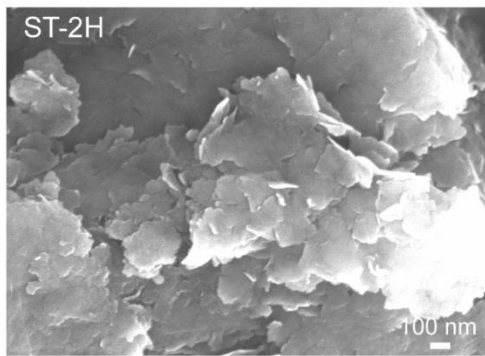


Figure S2: ^1H direct polarization MAS NMR spectrum of sodium acetate.

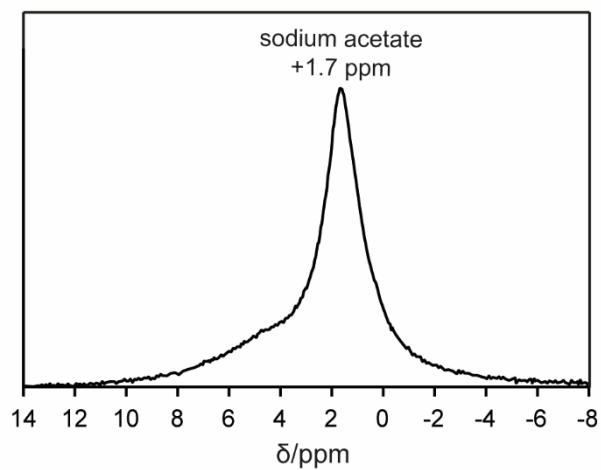


Figure S3: $\{^1\text{H}\} - ^{13}\text{C}$ HETCOR spectra of ST-AcONa.

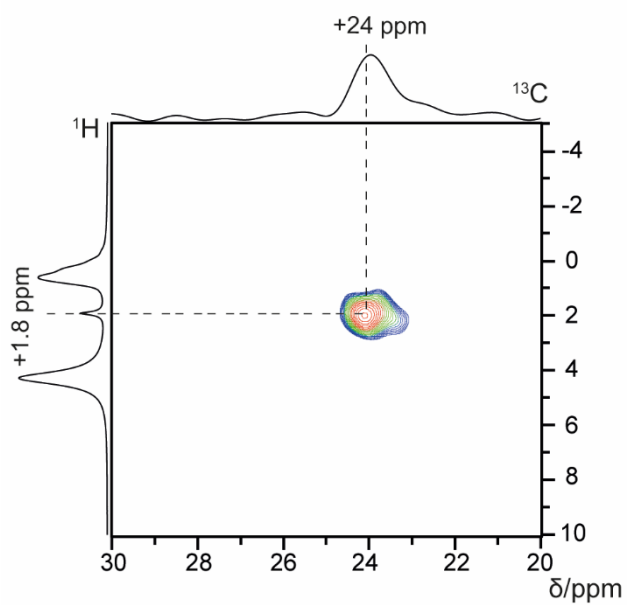


Figure S4: Example of deconvolution of a ^1H DP MAS-NMR

This figure shows the various contributions obtained by deconvolution of the ^1H DP MAS-NMR spectrum of ST-2H within the range of +1.5 ppm to -1.0 ppm. The exact peak positions may vary a little from one sample to another.

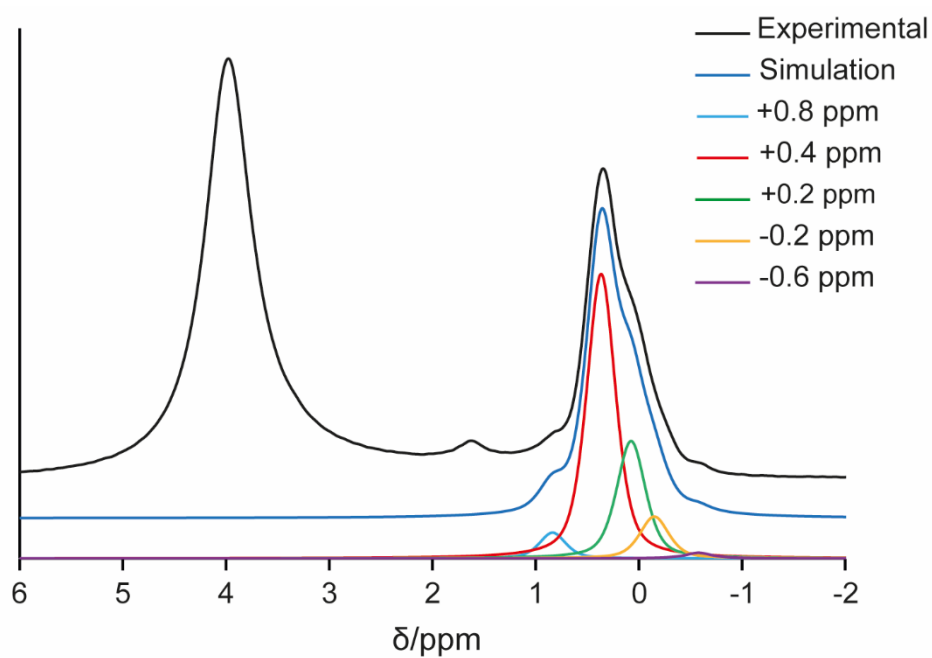


Figure S5: Slab model for the fully hydrated (130) talc edge: (a) side view, (b) top view, (c) front view, (d) perspective view.

This slab includes one TOT layer of width 4 tetrahedra. Atomic positions fully relaxed as a result from DFT simulation. The fully hydrated surface is covered by 10 water molecules per (130) face of one unit-cell of this slab model, i.e. normal to the slab unit-cell \vec{c} axis, 4 of which dissociatively chemisorbed on surface Si atoms, and 6 molecularly chemisorbed on surface Mg atoms

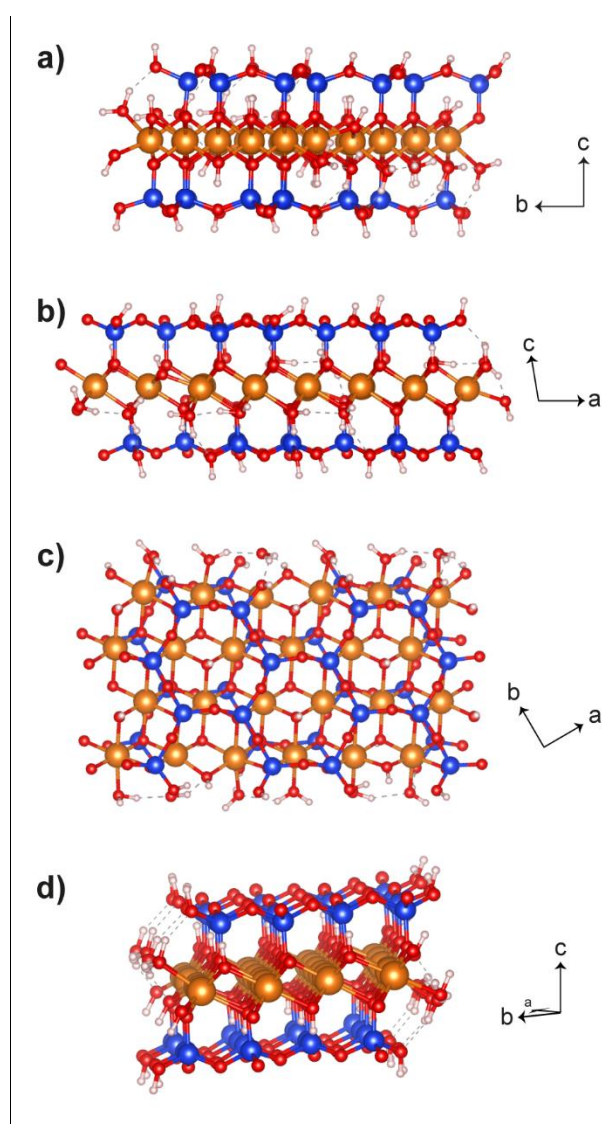


Figure S6: Slab model for the fully hydrated (100) talc edge: (a) side view, (b) top view, (c) front view, (d) perspective view.

This slab includes one TOT layer of width 3 tetrahedra. Atomic positions fully relaxed as a result from DFT simulation. The fully hydrated surface is covered by 5 water molecules per (100) face of one unit-cell of this slab model, i.e. normal to the slab unit-cell \vec{c} axis, 2 of which dissociatively chemisorbed on surface Si atoms, and 3 molecularly chemisorbed on surface Mg atoms.

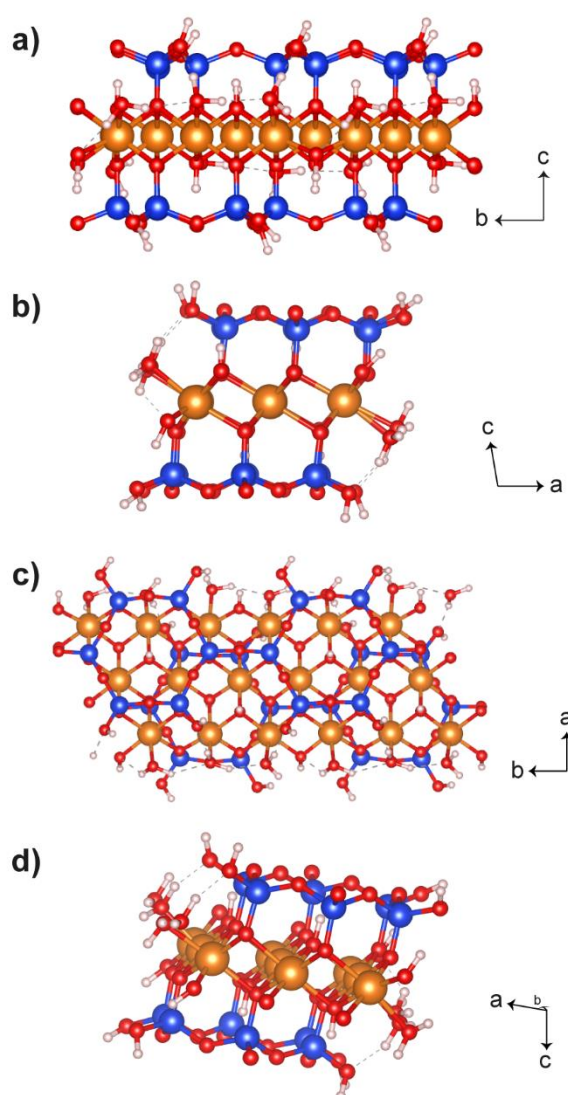


Figure S7: ^1H DQ-SQ PC7 spectrum of ST-6H.

The ^1H DQ-SQ PC7 spectrum shows contributions between 1-2 ppm (in the SQ dimension) and 2-4 ppm (in the DQ dimension) which indicate the presence of silanols groups in very small quantity in the ST-6H sample.

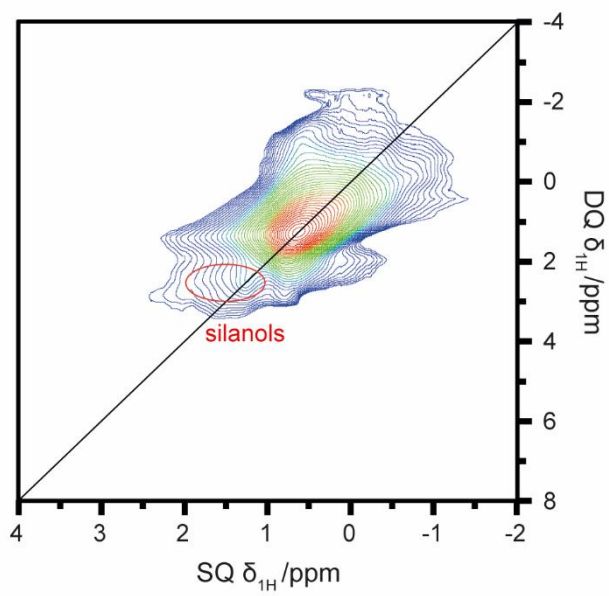
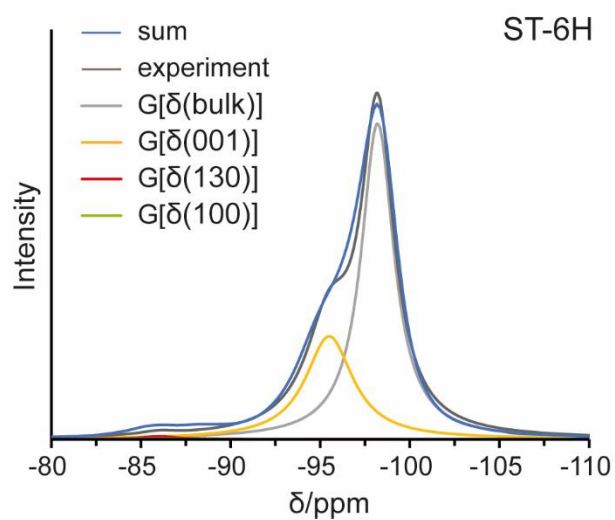
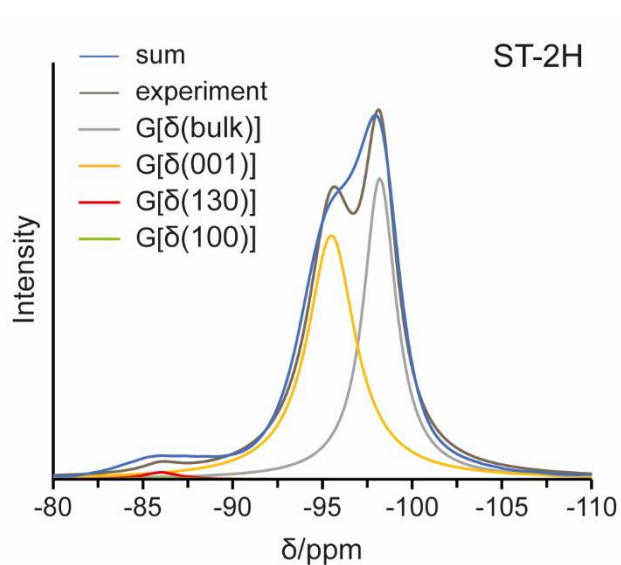
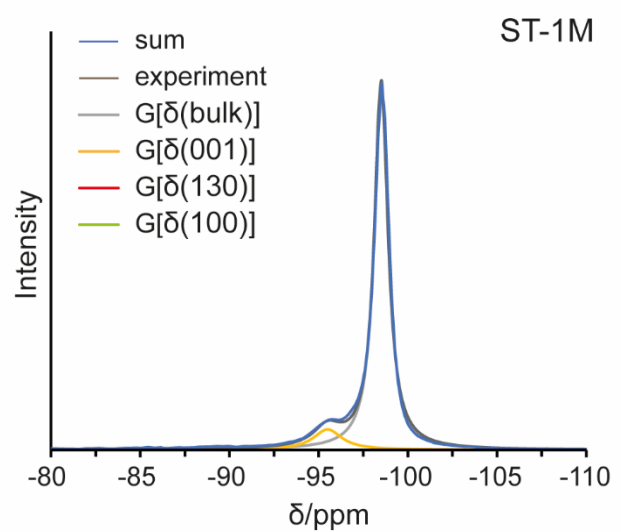
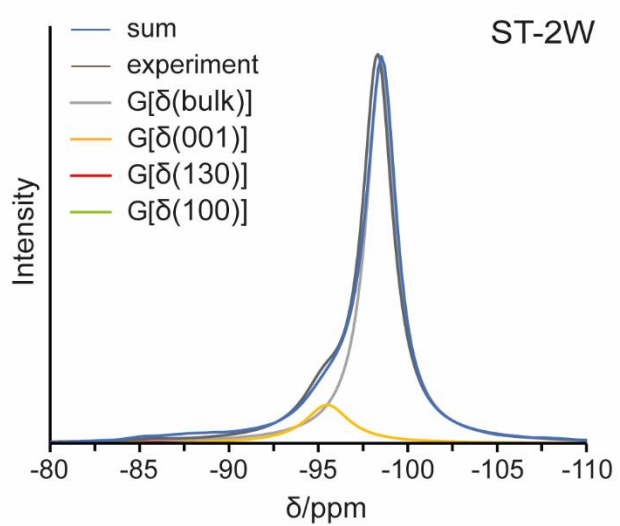
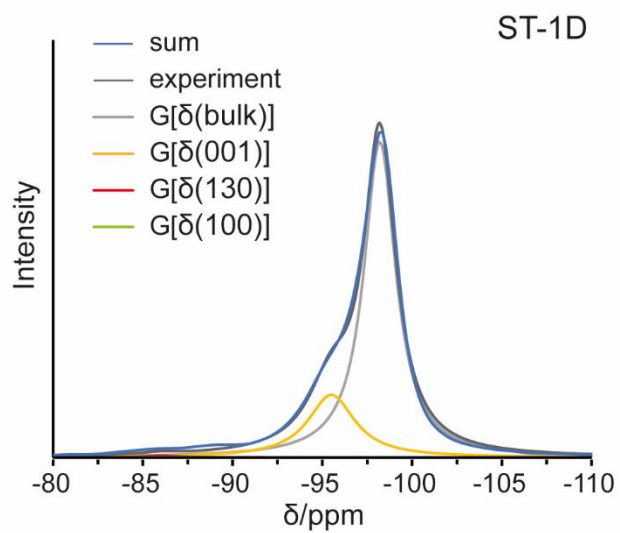


Figure S8: Decompositions of ^{29}Si NMR chemical shifts profiles

The figures presented in this section present distribution of NMR signals as function of ^{29}Si NMR chemical shift referenced to tetramethylsilane (TMS), in ppm. The experimental signal is normalized by its integral. Simulated contributions of the bulk and (001), (130), and (100) facets of talc nanocrystals sum up to a simulated normalized signal of integral 1. The nomenclature of samples is the same as in main text (e.g. ST-2H: Synthesis Time 2 hours, 6H 6 hours, 1D 1 day, 2W 2 weeks, 1 M 1 month, 2W-F fines fraction from centrifugation of ST-2W, 2W-C coarse fraction from centrifugation of ST-2W).





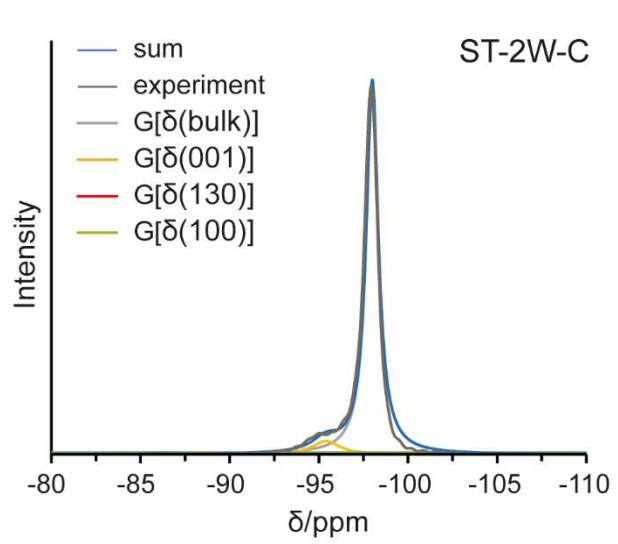
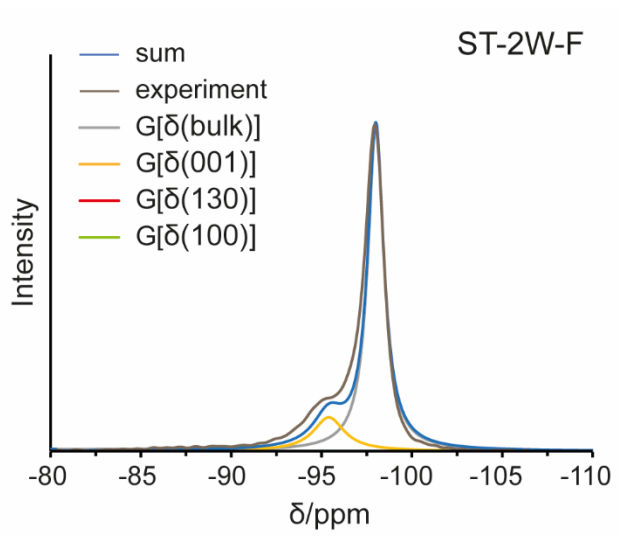


Figure S9: Variation of Log-normal talc nanoparticle size distributions parameters with synthesis time.

Figure S9a: Variation of the mean talc nanoparticle thickness with synthesis time.

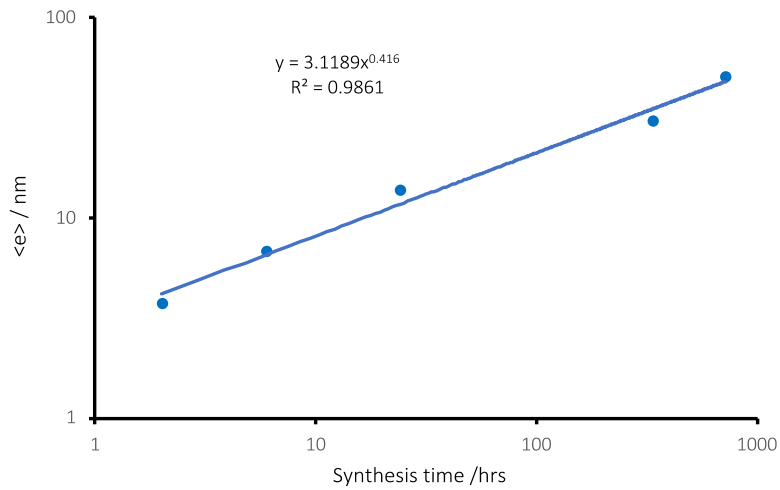


Figure S9b: Variation of the log-normal distribution parameter μ with time of synthesis

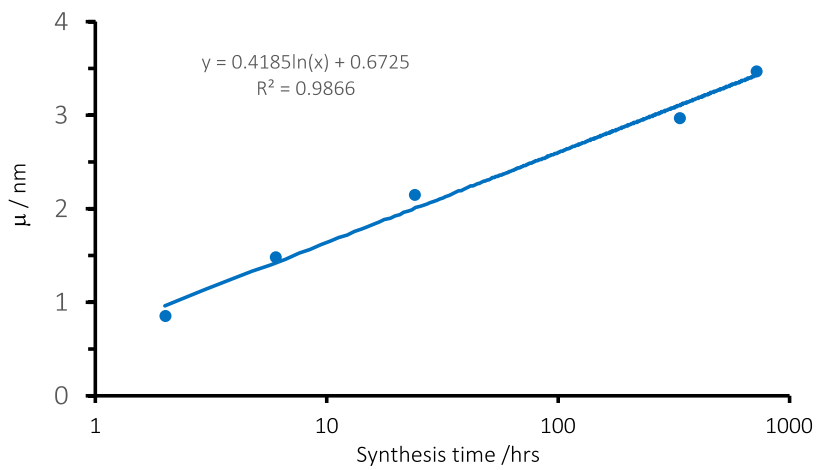
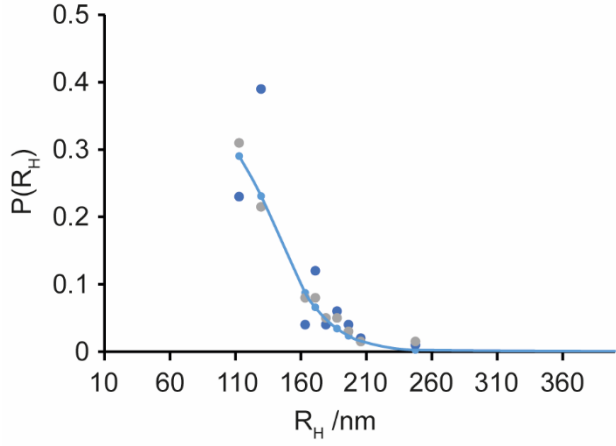


Figure S10: Example of lognormal distribution fitting DLS data of ST-2W.

On the figure presented, the raw DLS data are the blue dots, the grey dots are the moving averages of period 2 classes, and the blue line is the log-normal distribution fitted on the moving averaged data.

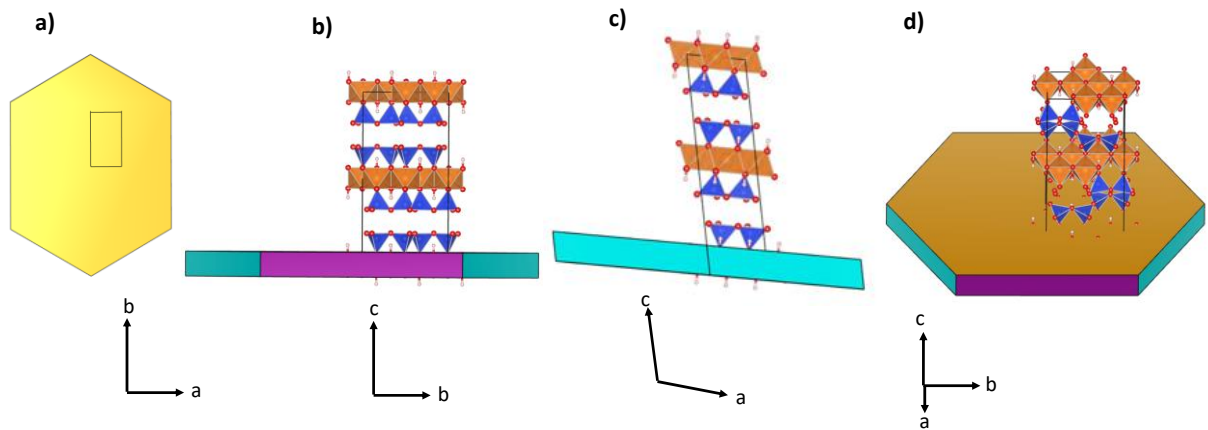


3 – Supporting calculations

3-1 Calculation of the hydrodynamic radius of a talc nanocrystallite at equilibrium morphology

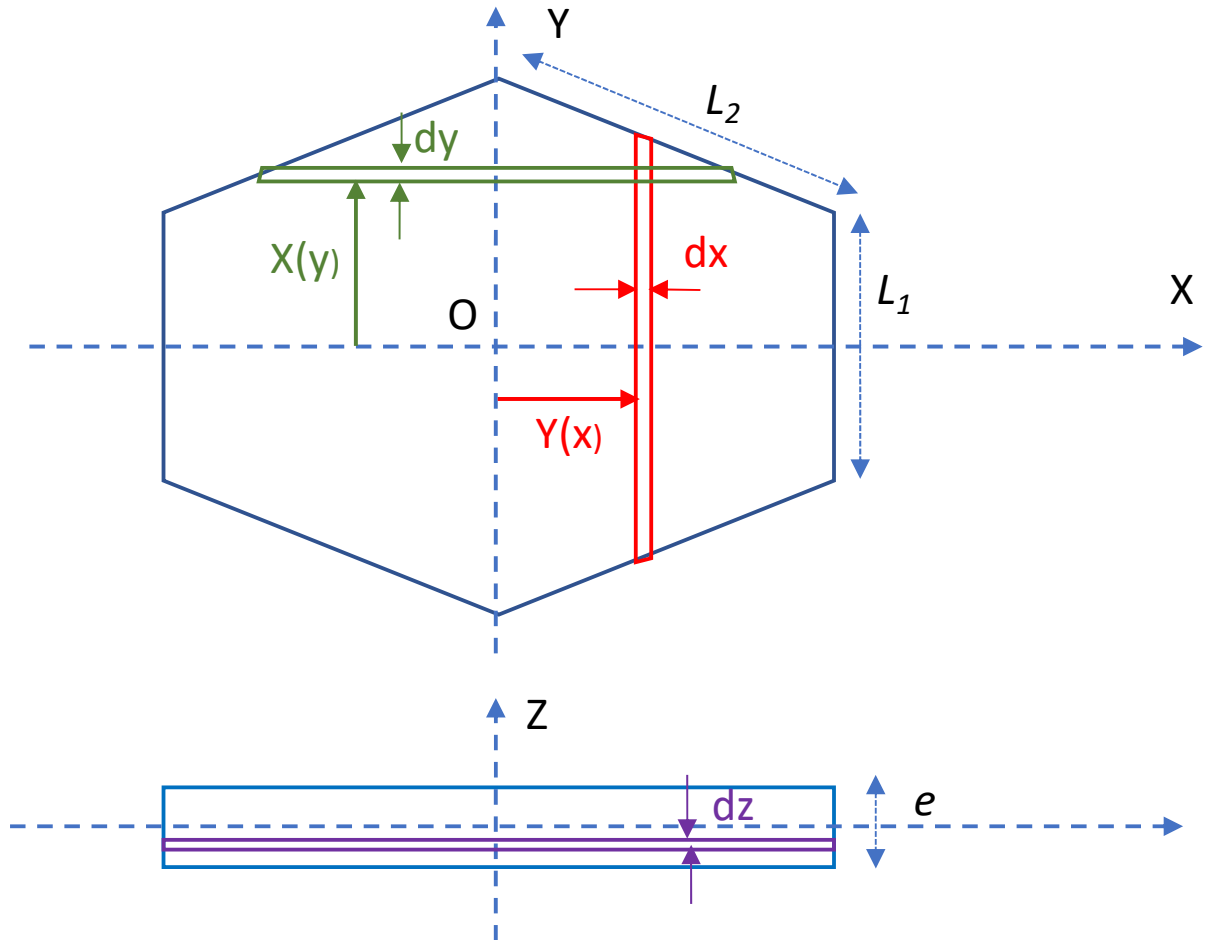
A crystallite of talc at equilibrium morphology in presence of liquid water and synthesis temperature (600K) expresses facets (001), (130) and (100) forming an irregular hexagonal prism as represented on Figure 9 of main text, reproduced hereafter for convenience:

Equilibrium morphology of a fully hydrated talc crystallite: (a) view along $-\vec{c}$ axis; (b) view along $-\vec{a}$ axis; (c) view along $-\vec{b}$ axis; (d) perspective view. Color code: facets (001) light orange, facets (130) light blue, facets (100) purple; polyhedral T in TOT layers blue, O in TOT layer orange, oxygen atoms red, hydrogen atoms light grey.



Its 6 summit angles are equal to $\pi/3$, and its shape is then fully determined by its thickness e and lengths L_1 and L_2 of facets (100) and (130) respectively. Thickness e can be chosen to fix the spatial scale, and lengths L_1 and L_2 at equilibrium morphology at any scale will obey equations (13) and (14) of main text, i.e. set in fixed proportions.

Let us compute the radius of gyration about its center of gravity of such a solid particle assumed homogeneous, as function of e , L_1 , L_2 and density ρ . The following scheme summarizes our notations:



We compute first the moments of inertia I_{yz} , I_{zx} , I_{xy} about planes yz, zx, and xy:

$$I_{yz} = 2 \int_0^{L_2 \cos(\pi/6)} x^2 dm \quad (\text{SI-1})$$

Where:

$$dm = \rho e Y(x) dx \quad (\text{SI-2})$$

and:

$$Y(x) = \left[L_1 + L_2 \left(1 - \frac{2x}{L_2 \sqrt{3}} \right) \right] \quad (\text{SI-3})$$

Therefore:

$$I_{yz} = 2\rho e \left[\int_0^{L_2 \sqrt{3}/2} (L_1 + L_2) x^2 dx - \frac{2}{\sqrt{3}} \int_0^{L_2 \sqrt{3}/2} x^3 dx \right] \quad (\text{SI-4})$$

or

$$I_{yz} = 2\rho e \left[\frac{(L_1+L_2)}{3} \left(\frac{L_2\sqrt{3}}{2} \right)^3 - \frac{2}{4\sqrt{3}} \left(\frac{L_2\sqrt{3}}{2} \right)^4 \right] \quad (\text{SI-5})$$

$$I_{yz} = 2\rho e \left(\frac{L_2\sqrt{3}}{2} \right)^3 \left[\left(\frac{L_1+L_2}{3} \right) - \frac{L_2}{4} \right] \quad (\text{SI-6})$$

and finally:

$$I_{yz} = \frac{\rho e L_2^3 \sqrt{3}}{16} (4L_1 + L_2) \quad (\text{SI-7})$$

Similarly:

$$I_{xz} = 2\rho \int X(y) y^2 dy \quad (\text{SI-8})$$

Where:

$$\text{for } y \in [0, L_1/2[, X(y) = X_1(y) = L_2\sqrt{3} \quad (\text{SI-9})$$

$$\text{and for } y \in \left[\frac{L_1}{2}, \frac{(L_1+L_2)}{2} \right] , X(y) = X_2(y) = 2\sqrt{3} \left[\frac{(L_1+L_2)}{2} - y \right] \quad (\text{SI-10})$$

so that:

$$I_{xz} = 2\rho e \left[\int_0^{L_1/2} L_2\sqrt{3} y^2 dy + \int_{L_1/2}^{(L_1+L_2)/2} 2\sqrt{3} \left[\frac{(L_1+L_2)}{2} - y \right] y^2 dy \right] \quad (\text{SI-11})$$

Therefore:

$$I_{xz} = 2\rho e \left[\frac{L_2\sqrt{3}}{3} \left(\frac{L_1}{2} \right)^3 + \frac{(L_1+L_2)}{\sqrt{3}} \left[\left(\frac{L_1+L_2}{2} \right)^3 - \left(\frac{L_1}{2} \right)^3 \right] - \frac{\sqrt{3}}{2} \left[\left(\frac{L_1+L_2}{2} \right)^4 - \left(\frac{L_1}{2} \right)^4 \right] \right] \quad (\text{SI-12})$$

or:

$$I_{xz} = 2\rho e \left[\left(\frac{L_1}{2} \right)^3 \left[\frac{-L_1}{4\sqrt{3}} \right] + \left(\frac{L_1+L_2}{2} \right)^4 \left[\frac{1}{2\sqrt{3}} \right] \right] \quad (\text{SI-13})$$

And rearranging:

$$I_{xz} = \frac{\rho e}{\sqrt{3}} \left[\left(\frac{L_1 + L_2}{2} \right)^4 - \left(\frac{L_1}{2} \right)^4 \right] \quad (\text{SI-14})$$

or:

$$I_{xz} = \frac{\rho e L_2 (L_1 + 2L_2)}{4\sqrt{3}} \left[\left(\frac{L_1 + L_2}{2} \right)^2 + \left(\frac{L_1}{2} \right)^2 \right] \quad (\text{SI-15})$$

Lastly:

$$I_{xy} = 2A\rho \int_0^{e/2} z^2 dz = \rho e A \frac{e^2}{12} \quad (\text{SI-16})$$

Where:

$$A = \frac{L_2 \sqrt{3}}{2} (2L_1 + L_2) \quad (\text{SI-17})$$

is the basal area. Let us express further the mass M of the crystallite:

$$M = \rho e A \quad (\text{SI-17})$$

Let us now express the 3 moments of inertia about axes , y , z :

$$I_x = I_{zx} + I_{xy} \quad (\text{SI-18})$$

$$I_y = I_{yx} + I_{zy} \quad (\text{SI-18})$$

$$I_z = I_{zx} + I_{zy} \quad (\text{SI-18})$$

The moment of inertia about the center of mass O is:

$$I_O = \frac{I_x + I_y + I_z}{3} \quad (\text{SI-19})$$

and the corresponding radius of gyration:

$$R_O = \sqrt{\frac{I_O}{M}} \quad (\text{SI-20})$$

Therefore:

$$I_x = M \left[\frac{(L_1+2L_2)}{6(2L_1+L_2)} \left[\left(\frac{L_1+L_2}{2} \right)^2 + \left(\frac{L_1}{2} \right)^2 \right] + \frac{e^2}{12} \right] \quad (\text{SI-21})$$

$$I_y = M \left[\frac{L_2^2(4L_1+L_2)}{8(2L_1+L_2)} + \frac{e^2}{12} \right] \quad (\text{SI-22})$$

$$I_z = M \left[\frac{(L_1+2L_2)}{6(2L_1+L_2)} \left[\left(\frac{L_1+L_2}{2} \right)^2 + \left(\frac{L_1}{2} \right)^2 \right] + \frac{L_2^2(4L_1+L_2)}{8(2L_1+L_2)} \right] \quad (\text{SI-23})$$

And therefore:

$$R_O = \left[\frac{2}{3} \left(\frac{(L_1+2L_2)}{6(2L_1+L_2)} \left[\left(\frac{L_1+L_2}{2} \right)^2 + \left(\frac{L_1}{2} \right)^2 \right] + \frac{L_2^2(4L_1+L_2)}{8(2L_1+L_2)} + \frac{e^2}{12} \right) \right]^{1/2} \quad (\text{SI-24})$$

Let us now assume $L_1 = \alpha e$ and $L_2 = \beta e$, the previous equation becomes:

$$R_O = e \left[\frac{2}{3} \left(\frac{(\alpha+2\beta)}{6(2\alpha+\beta)} \left[\left(\frac{\alpha+\beta}{2} \right)^2 + \left(\frac{\alpha}{2} \right)^2 \right] + \frac{\beta^2(4\alpha+\beta)}{8(2\alpha+\beta)} + \frac{1}{12} \right) \right]^{1/2} \quad (\text{SI-25})$$

R_O is identical to the hydrodynamic radius R_H under the assumption that there are no strongly adsorbed solvent molecules contributing to the nanoparticle inertia. Taking $\alpha = 8.176$ and $\beta = 6.013$ from equation (13) and (14) at the equilibrium morphology of hydrated talc at 600K, we get:

$$R_H \approx 3.464 e \quad (\text{SI-26})$$